J. Synchrotron Rad. (1998). **5**, 398–400

A dynamic local bump system for producing synchrotron radiation with an alternating elliptical polarization

K. K. Lin,* K. T. Hsu, J. S. Chen, C. H. Kuo, C. S. Chen, K. H. Hwu, J. Chen, K. T. Pan, C. J. Wang, J.-R. Chen and C. T. Chen

Synchrotron Radiation Research Center, Hsinchu 300, Taiwan. E-mail: kklin@srrc09.srrc.gov.tw

(*Received 4 August 1997; accepted 6 October 1997*)

To facilitate high-sensitivity soft X-ray magnetic circular dichroism experiments, a dynamic local bump system has been developed at the SRRC storage ring. This system was devised to vary dynamically the vertical slope of the electron beam in a bending magnet, producing, in the electron orbit plane, soft X-rays with an alternating elliptical polarization. The local bump was created by using two pairs of vertical correctors located on each side of the bending magnet. The bump strength coefficient was obtained both from calculated estimation and from measured beam-response matrices. Control electronics for proper bump strength settings were designed to incorporate the existing orbit-corrector function. A corresponding graphic user interface was implemented so that the bump amplitude could be easily adjusted. The performance of this system is presented. Disturbance on the stored electron beam orbit was observed while flipping the corrector polarity during EPBM (elliptical polarization from bending magnets) operation. A local feedback loop, developed to eliminate such disturbance on other beamlines, is also described.

Keywords: elliptical polarization from bending magnets (EPBM); local bump; dynamics.

1. Introduction

The prospect of obtaining element- and site-specific magnetic information has stimulated a good number of experiments taking advantage of circularly polarized synchrotron radiation (Schutz *et al.*, 1987; Chen *et al.*, 1990; Koide *et al.*, 1991). These magnetic circular dichroism (MCD) experiments, whether performed in absorption or reflection, offer the possibility of determining the magnetic moment of each element in the material being investigated. In addition, it is possible to dissect further the magnetic moment into spin and orbit contributions (Chen *et al.*, 1995), to determine the magnetic profile of multilayers including interfacial magnetic roughness (Kao *et al.*, 1994), and to measure element-specific magnetic hysteresis curves (Chen *et al.*, 1993). To increase the sensitivity and to facilitate high-field soft X-ray MCD measurements using bending magnets, we have designed and constructed a local bump system which can alternate the elliptical polarization from bending magnets (EPBM). Although the basic principle of EPBM is very similar to that of elliptically polarized wigglers (Randall *et al.*, 1996), EPBM can provide photons with a much purer polarization state and has a greater MCD measuring sensitivity.

It is planned to have an EPBM operation mode which provides adjustable degrees of polarization with a polarity-switching frequency of a few Hz.

2. Technical features

2.1. *Principle and spatial arrangement*

A schematic illustration of EPBM operation is shown in Fig. 1. The SRRC storage ring lattice structure is a triple-bend achromat with sixfold symmetry (Kuo *et al.*, 1994) and the EPBM beamline is situated at the second bending magnet of the third-section achromat. As shown in the figure, the electron beam trajectory can be either flipped up or down depending on the bump magnet polarity chosen. When the electrons are moving along the tilted-up beam trajectory, the downstream beamline receives left-elliptically polarized radiation emitted just below the local beam trajectory. As the bump polarity changes, the beam path is flipped to trace out the tilted-down trajectory such that the downstream beamline receives right-elliptically polarized radiation emitted just above the local beam trajectory.

One set of four vertical correctors was chosen to generate this local bump. Locations for installing these extra correction magnets were limited by the existing elements in the lattice structure. A compromised solution ended up with the arrangement shown in Fig. 1. Each corrector is capable of providing 1.7 mrad deflection on the stored 1.5 GeV electron beam. The estimated available tilt angle of the electron beam at the photon extraction point is about 0.25 mrad.

2.2. *Bump coefficient determination*

With a specified user shift machine lattice, the bump coefficients can be experimentally determined by using the measured beam-response matrix, and various beam trajectory bumps can be readily generated in a similar way. Bump shape adjustment will provide the capability of convenient tuning in future beamline commissioning.

The estimated bump coefficients can be verified under DC mode operation and some fine adjustment may be needed in practice. In DC mode operation, the EPBM bump was generated and its influence on the beam orbit change was monitored. An example of a DC local bump is shown in Fig. 2. A local bump in the R3BM2 region is added onto the regular user shift beam trajectory along the storage ring.

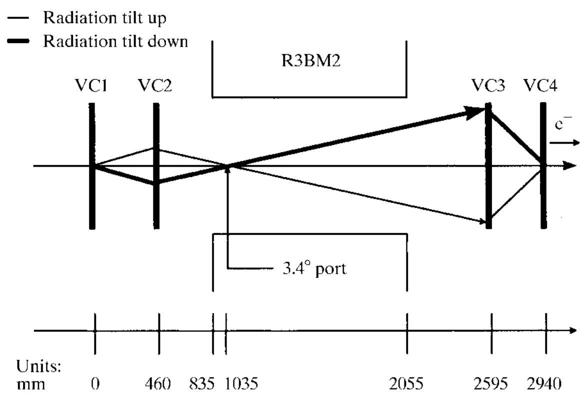

Figure 1
Operational schematic illustration of the EPBM system.

3. Implementation and test results

3.1. *Control electronics and graphic user interface*

A functional block diagram of the electronics is given in Fig. 3. As shown in the figure, these dynamic local bump magnets can also act as correction magnets. In switching the local bump polarity, a ramp generator was applied so as to keep the polarity transient duration longer than the magnet response time of 25 ms. Tuning of the bump amplitude, which is directly related to the degree of polarization, was achieved by adjusting the bump amplitude control knob, and the polarity switching frequency was determined by an external square-wave-function generator.

The EPBM graphic user interface was designed to provide easy adjustment of the degree of polarization. The EPBM control page is shown in Fig. 4. Tuning knob settings of the bump coefficient for four magnets were determined from measured response matrices.

3.2. *Mismatch of the eddy current effect due to a bellow in the third corrector and its phase compensation*

When the EPBM was tested in AC mode, beam orbit disturbance was observed outside the EPBM local bump. It was found that the beam orbit disturbance occurred during the transience of the bumper polarity change. The vertical beam position at some of the beam-position monitors located outside the EPBM bump may give a beam position shift as large as 150 µm for 40 ms duration. This 40 ms period corresponds to the transient duration set by the control electronics. The amplitude of this beam position shift depends on the bump strength applied and matching among bumper magnets. A major source of causing this mismatching was due to a bellow-type vacuum chamber located inside the third bumper magnet. The different response among the other three (magnet–vacuum) combinations may contribute to this disturbance as well. In order to overcome this difficulty, a compensation circuit was built into the control electronics for the third magnet channel to compensate the mismatch due to the eddy current effect, and the beam position shift amplitude was reduced to one-fifth of its original value.

3.3. *Beam test result with local feedback loop*

Although the compensator in the EPBM control electronics provides a reduction in the orbit disturbance on the beam orbit during the polarity transient period, further improvement is still desirable. A local feedback loop on the beamline of interest was put to test in stabilizing the beam trajectory upstream of the beamline. As illustrated in Fig. 5, with EPBM control electronics operating at 0.5 Hz, a local feedback loop was set up for stabilizing the R2BM3 beamline, whereas the EPBM beamline is located downstream of R3BM2. The beam test result is shown in Fig. 6. As shown in the figure, beam-position monitors within the region of the applied feedback loop (R2BPM5Y, R2BPM6Y) and

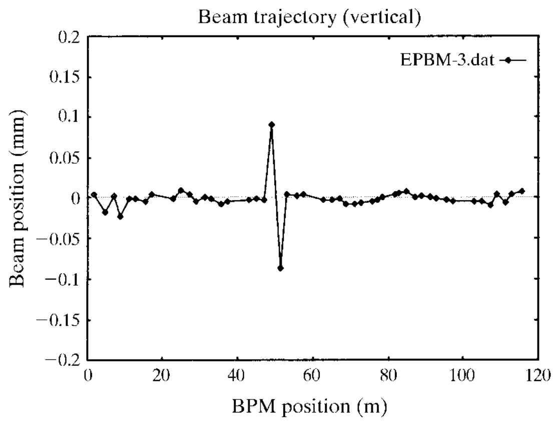

Figure 2
A typical local bump was generated in the third-section storage ring under regular user shift lattice.

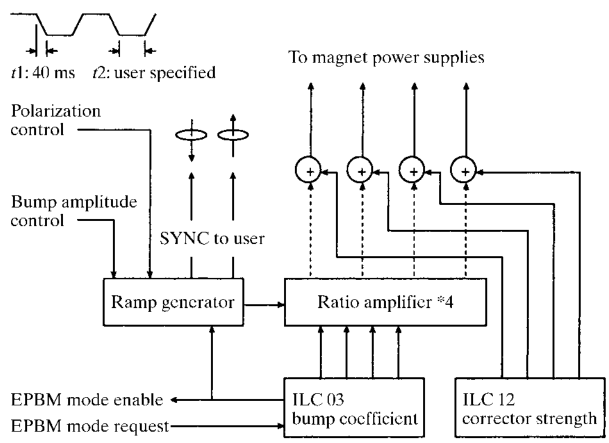

Figure 3
Functional block diagram of the EPBM control electronics.

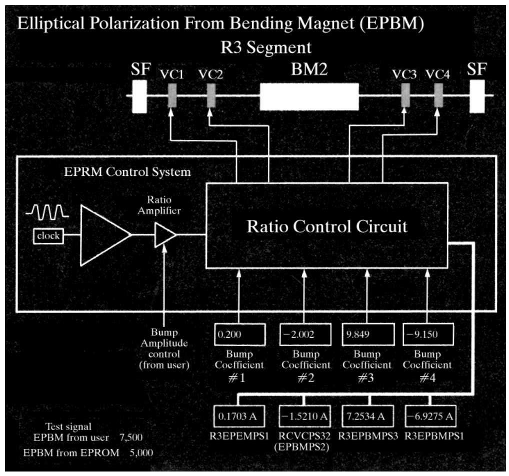

Figure 4
Display of the present phase EPBM graphic user interface.

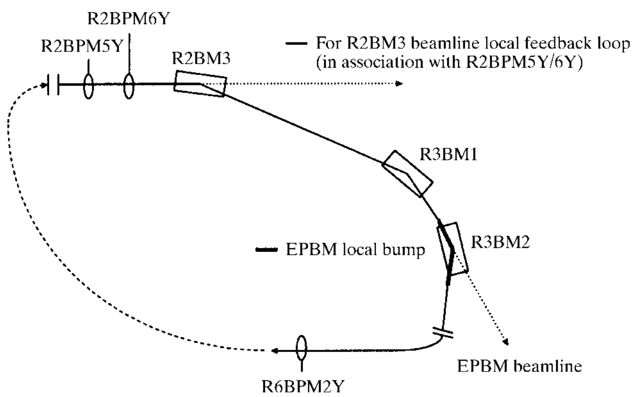

Figure 5
Schematic layout of the test run of the EPBM with local feedback loop.

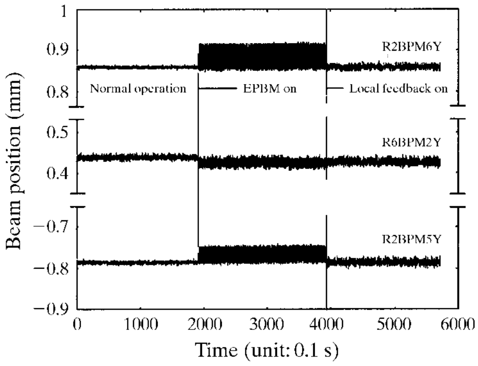

Figure 6
Monitoring beam position fluctuation while the EPBM is operating and then is suppressed by the local feedback loop.

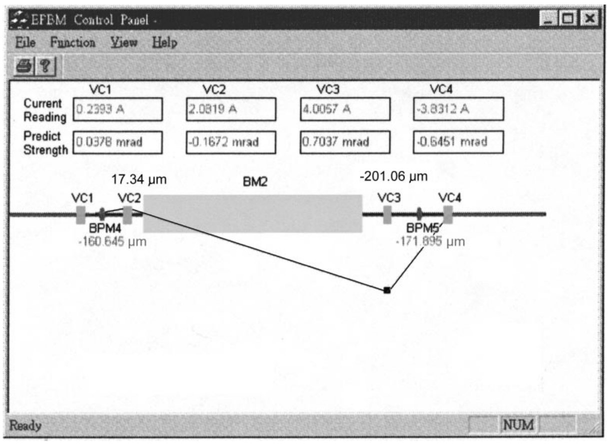

Figure 7
Preliminary PC version of the EPBM graphic user interface for end-station users.

the outside one (R6BPM2Y) give the beam position during this experiment. At the beginning of this experiment, beam position readings were recorded under the normal operation mode. Then, the EPBM control electronics were turned on in order to observed its influence on the beam position fluctuation at upstream beam-position monitors of a selected beamline. The local feedback loop was turned on 3 min later in order to suppress the beam position fluctuation induced by EPBM operation.

This experimental result indicates that, with the EPBM in operation, other beamlines may be disturbed by the EPBM local bump mismatch during flipping of the correctors polarity. Beam position fluctuations of 40 µm (R2BPM5Y), 70 µm (R2BPM6Y) and 30 µm (R6BPM2Y) were observed while the EPBM was operating. This implies that beamlines located downstream of R2BPM5Y/R2BPM6Y and that of R6BPM2Y were greatly disturbed by this EPBM operation. However, when a local feedback loop installed in the region where R2BPM5Y/R2BPM6Y is located was turned on, the beam position was stabilized to have a fluctuation within 15 µm, 15 µm and 25 µm, respectively. This indicates that installing the local feedback loop at the beamlines of interest (in this case it is the R2BM3 beamline) can be a great help in stabilizing the upstream beam position.

4. Improvement

Some test runs have been carried out recently in order to improve the EPBM operation performance.

(i) Fine tuning of the amplitude and the phase compensation circuit on the third corrector channel has been tested. With few iterations, the orbit shifted amplitude was reduced to about one-eighth of its original value.

(ii) As shown in Fig. 7, a preliminary personal computer graphic user interface was developed. It is one of the possible options of providing easy adjustment and orbit-bump-related information for end-station users.

(iii) The current amplifier was bench tested and was capable of reducing the transient duration to 10 ms in switching magnet polarity. Therefore the switching frequency can be increased.

References

Chen, C. T., Idzerda, Y. U., Lin, H. G., Meigs, G., Chaiken, A., Prinz, G. A. & Ho, G. H. (1993). *Phys. Rev. B*, **48**, 642–645.

Chen, C. T., Idzerda, Y. U., Lin, H. J., Smith, N. V., Meigs, G., Chaban, E., Ho, G. H., Pellegrin, E. & Sette, F. (1995). *Phys. Rev. Lett.* **75**, 152–155.

Chen, C. T., Sette, F., Ma, Y. & Modesti, S. (1990). *Phys. Rev. B*, **42**, 7262–7265.

Kao, C.-C., Chen, C. T., Johnson, E. D., Hastings, J. B., Lin, H. J., Ho, G. H., Meigs, G., Brot, J.-M., Hulbert, S. L., Idzerda, Y. U. & Vettier, C. (1994). *Phys. Rev. B*, **50**, 9599–9602.

Koide, T., Shidara, T., Fukutani, H., Yamaguchi, K., Fujimori, A. & Kimura, S. (1991). *Phys. Rev. B*, **44**, 4697–4700.

Kuo, C. C., Hsu, K. T., Chang, H. P., Travier, C., Jan, G. J. & Hsue, C. S. (1994). *Conference Proceedings of EPAC94*, pp. 1018–1020, London, UK.

Randall, K. J., Xu, Z., Gluskin, E., McNulty, I., Dejus, R., Krinsiy, S., Singh, Q. V., Kao, C.-C., Johnson, E. D., Chen, C. T. & Meigs, G. (1996). *J. Electron. Spectrosc. Relat. Phenom.* **80**, 433–436.

Schutz, G., Wagner, W., Wilhelm, W., Kienle, P., Zeller, R., Frahm, R. & Materlik, G. (1987). *Phys. Rev. Lett.* **58**, 737–740.